A CCD-ADI method for unsteady convection-diffusion equations ☆

Hai-Wei Sun*, Leonard Z. Li

Department of Mathematics, University of Macau, Macao

Abstract

With a combined compact difference scheme for the spatial discretization and the Crank-Nicolson scheme for the temporal discretization, respectively, a high-order alternating direction implicit method (ADI) is proposed for solving unsteady two dimensional convection-diffusion equations. The method is sixth-order accurate in space and second-order accurate in time. The resulting matrix at each ADI computation step corresponds to a triple-tridiagonal system which can be effectively solved with a considerable saving in computing time. In practice, Richardson extrapolation is exploited to increase the temporal accuracy. The unconditional stability is proved by means of Fourier analysis for two dimensional convection-diffusion problems with periodic boundary conditions. Numerical experiments are conducted to demonstrate the efficiency of the proposed method. Moreover, the present method preserves the higher order accuracy for convection-dominated problems.

Keywords: unsteady convection-diffusion equation, combined compact difference scheme, alternating direction implicit method, unconditionally stable

1. Introduction

In this paper, we study the unsteady two dimensional (2D) convection-diffusion equation for a transport variable u,

$$\frac{\partial u}{\partial t} - a\frac{\partial^2 u}{\partial x^2} - b\frac{\partial^2 u}{\partial y^2} + p\frac{\partial u}{\partial x} + q\frac{\partial u}{\partial y} = S(x,y,t),\ (x,y,t) \in \Omega \times (0,T], \tag{1}$$

with the initial condition

$$u(x,y,0) = u_0(x,y),\ (x,y) \in \Omega, \tag{2}$$

and the boundary condition

$$u(x,y,t) = g(x,y,t),\ (x,y) \in \partial\Omega,\ t \in (0,T], \tag{3}$$

☆The research was partially supported by the research grant 005/2012/A1 from FDCT of Macao, and MYRG140(Y3-L2)-FST11-SHW from University of Macau.

*Corresponding author

Email addresses: HSun@umac.mo (Hai-Wei Sun), reachless@live.cn (Leonard Z. Li)

where Ω is a rectangular domain in $\mathbb{R}^2$, $\partial\Omega$ is the boundary of Ω, (0,T] is the time interval, u_0, the source term S, and g are given sufficiently smooth functions, p and q are constant velocities of convection, and a, $b > 0$ are constant diffusion coefficients in x- and y-directions, respectively. For its relevance to various practical applications, (1) can be used to model many phenomena in the physical sciences relating to the convection and diffusion of various physical quantities, such as mass, heat, energy, and vorticity [11]. It also plays an important role in computational fluid dynamics [3, 14].

Many attempts have been made to develop finite difference methods with better properties for the numerical solution of unsteady convection-diffusion problems. Among these methods, the alternating direction implicit (ADI) method proposed by Peaceman and Rachford [10] is well-known and popular for its high efficiency. The main idea of the ADI method is converting a multi-dimensional problem into a collection of one-dimensional problems, which usually only require tridiagonal matrices to be dealt with. Nevertheless, their method is second order accurate in space and may produce considerable dissipation and phase errors. To obtain higher order accurate solutions, one needs to adopt higher order schemes for spatial approximations.

In the last two decades or so, higher order compact (HOC) schemes, which lead to higher order accurate approximations with smaller stencils, have been widely utilized for steady problems [6, 12]. In 2004, Karaa and Zhang [5] proposed an HOC scheme with the ADI (HOC-ADI) method for solving 2D unsteady convection-diffusion equations. Their method, which is fourth-order accurate in space and second-order accurate in time, with the computational efficiency of the ADI approach, is unconditionally stable. Tian [14] derived a rational HOC scheme with ADI (RHOC-ADI) method, which is unconditionally stable with fourth-order accuracy in space and second-order accuracy in time, and has better phase and amplitude error properties than the HOC-ADI scheme in [5]. Besides [5, 14], many other HOC-ADI methods for 2D convection-diffusion equations have also been proposed [4, 7, 8, 15, 16, 17]. Nevertheless, there are no discussions for extremely convection-dominated cases by HOC-ADI schemes in the literature. Indeed, for 2D convection-diffusion equations, when convection coefficients are gradually dominant, the accuracy of approximations by the HOC-ADI method [5] or the RHOC-ADI method [14] will be generally lost; see section 4.

The combined compact difference (CCD) method was proposed by Chu and Fan [1] for solving 1D and 2D steady convection diffusion equations. The CCD method is an implicit three-point scheme with sixth-order accuracy which can be efficiently solved by the so-called triple-tridiagonal solver [1]. Along with the ADI method, in this paper, we develop a CCD-ADI method to solve the 2D unsteady convection-diffusion equation (1). More precisely, we first exploit the Crank-Nicolson method for the temporal discretization of (1), and factorize the semi-discretized equation into two 1D convection-diffusion equations by the ADI approach. Then the CCD method is employed to solve the resulting 1D convection-diffusion equations. Meanwhile, the fast triple-tridiagonal solver is involved. The CCD-ADI method can achieve sixth-order spatial accuracy and second-order temporal accuracy. In practice, the Richardson extrapolation can be exploited to increase the temporal accuracy to fourth-order, as in [8]. Numerical results show that the CCD-ADI method retains a better approximation even for the extremely convection-dominated problem.

The rest of the paper is organized as follows. In section 2, we derive the CCD-ADI scheme. The von Neumann linear stability analysis is carried out for the proposed CCD-ADI method in section 3. In section 4, numerical experiments are conducted to show the performance of the present method. Concluding remarks are given in section 5.

2. CCD-ADI scheme

For convenience, we define two operators

$$\mathcal{L}_x \equiv a\frac{\partial^2}{\partial x^2} - p\frac{\partial}{\partial x} \text{ and } \mathcal{L}_y \equiv b\frac{\partial^2}{\partial y^2} - q\frac{\partial}{\partial y}.$$

Thus the equation (1) can be written as

$$\frac{\partial u}{\partial t} = (\mathcal{L}_x + \mathcal{L}_y)u + S(x,y,t). \tag{4}$$

We first divide the time interval $[0,T]$ into N time steps, with the time increment $\Delta t = T/N$, and $t_n = n\Delta t$, $n = 0, 1, \dots, N$. Let v^α be the approximation of $v(x, y, \alpha\Delta t)$ for an arbitrary function $v(x, y, t)$ with a positive real number α. Using the Crank-Nicolson scheme around $t = t_n + \Delta t/2$ to discretize the time derivative in (4), we have

$$\frac{u^{n+1} - u^n}{\Delta t} = \frac{1}{2}(\mathcal{L}_x + \mathcal{L}_y)(u^{n+1} + u^n) + S^{n+1/2} + \mathcal{O}(\Delta t^2). \tag{5}$$

Collecting the terms for u^{n+1} and u^n in (5) leads to

$$\left(1 - \frac{\Delta t}{2}\mathcal{L}_x - \frac{\Delta t}{2}\mathcal{L}_y\right)u^{n+1} = \left(1 + \frac{\Delta t}{2}\mathcal{L}_x + \frac{\Delta t}{2}\mathcal{L}_y\right)u^n + \Delta t S^{n+\frac{1}{2}} + \mathcal{O}(\Delta t^3). \tag{6}$$

Since all coefficients in (1) are constant, (6) can be represented in the factored form

$$\begin{aligned}\left(1 - \frac{\Delta t}{2}\mathcal{L}_x\right)\left(1 - \frac{\Delta t}{2}\mathcal{L}_y\right)u^{n+1} &= \left(1 + \frac{\Delta t}{2}\mathcal{L}_x\right)\left(1 + \frac{\Delta t}{2}\mathcal{L}_y\right)u^n + \Delta t S^{n+1/2} \\ &\quad + \frac{\Delta t^2}{4}\mathcal{L}_x\mathcal{L}_y(u^{n+1} - u^n) + \mathcal{O}(\Delta t^3).\end{aligned} \tag{7}$$

Noting the fact that $u^{n+1} - u^n = \mathcal{O}(\Delta t)$, (7) is indeed

$$\left(1 - \frac{\Delta t}{2}\mathcal{L}_x\right)\left(1 - \frac{\Delta t}{2}\mathcal{L}_y\right)u^{n+1} = \left(1 + \frac{\Delta t}{2}\mathcal{L}_x\right)\left(1 + \frac{\Delta t}{2}\mathcal{L}_y\right)u^n + \Delta t S^{n+1/2} + \mathcal{O}(\Delta t^3). \tag{8}$$

In order to solve u^{n+1} in (8), operator forms of $[1 - (\Delta t/2)\mathcal{L}_x]$ and $[1 - (\Delta t/2)\mathcal{L}_y]$ must be inverted, which reduce to the solutions of 1D problems in x- and y- directions, respectively.

In the following, we briefly introduce the CCD method for solving 1D differential equation.

2.1. The CCD scheme

We start by considering the following 1D differential equation,

$$\alpha(x)\frac{d^2u}{dx^2} + \beta(x)\frac{du}{dx} + \gamma(x)u = f(x),\ 0 \le x \le L, \tag{9}$$

with the boundary condition

$$\zeta_1(x)u(x) + \zeta_2(x)u'(x) = c(x),\ x = 0,\ L, \tag{10}$$

where α, β, γ, f, ζ_1, ζ_2, and c are given functions.

Discretize the interval $[0, L]$ into a uniform grid $0 = x_0 < x_1 < \cdots < x_{M-1} < x_M = L$ with a spacing $h = L/M$. Using the Taylor expansion for an arbitrary function $v(x)$ at x_i, $i = 1, 2, \ldots, M-1$, with up to sixth derivative, we have

$$\begin{aligned} v(x_{i\pm1}) &= v(x_i) \pm hv'(x_i) + \frac{h^2}{2}v''(x_i) \pm \frac{h^3}{6}v^{(3)}(x_i) + \frac{h^4}{24}v^{(4)}(x_i) \pm \frac{h^5}{120}v^{(5)}(x_i) \\ &+\frac{h^6}{720}v^{(6)}(x_i) + \mathcal{O}(h^7). \end{aligned}$$

We substitute u, u', and u'' for v in the left-hand side of above Taylor expansion, respectively. By simple calculation, following two sets of equations are easily obtained,

$$\begin{cases} \dfrac{u(x_{i+1}) - u(x_{i-1})}{2h} &= u'(x_i) + \dfrac{h^2}{6}u^{(3)}(x_i) + \dfrac{h^4}{120}u^{(5)}(x_i) + \mathcal{O}(h^6), \\ \dfrac{u'(x_{i+1}) + u'(x_{i-1})}{2} &= u'(x_i) + \dfrac{h^2}{2}u^{(3)}(x_i) + \dfrac{h^4}{24}u^{(5)}(x_i) + \mathcal{O}(h^6), \\ u''(x_{i+1}) - u''(x_{i-1}) &= \quad 2hu^{(3)}(x_i) + \dfrac{h^3}{3}u^{(5)}(x_i) + \mathcal{O}(h^5), \end{cases} \tag{11}$$

and

$$\begin{cases} \dfrac{u(x_{i+1}) - 2u(x_i) + u(x_{i-1})}{h^2} &= u''(x_i) + \dfrac{h^2}{12}u^{(4)}(x_i) + \dfrac{h^4}{360}u^{(6)}(x_i) + \mathcal{O}(h^6), \\ \dfrac{u'(x_{i+1}) - u'(x_{i-1})}{2h} &= u''(x_i) + \dfrac{h^2}{6}u^{(4)}(x_i) + \dfrac{h^4}{120}u^{(6)}(x_i) + \mathcal{O}(h^6), \\ \dfrac{u''(x_{i+1}) + u''(x_{i-1})}{2} &= u''(x_i) + \dfrac{h^2}{2}u^{(4)}(x_i) + \dfrac{h^4}{24}u^{(6)}(x_i) + \mathcal{O}(h^6). \end{cases} \tag{12}$$

From (11) and (12), the first and second derivatives are expressed as

$$\begin{aligned} u'(x_i) &= \frac{15}{16h}[u(x_{i+1}) - u(x_{i-1})] - \frac{7}{16}[u'(x_{i+1}) + u'(x_{i-1})] \\ &+\frac{h}{16}[u''(x_{i+1}) - u''(x_{i-1})] + \mathcal{O}(h^6) \end{aligned} \tag{13}$$

and

$$u''(x_i) = \frac{3}{h^2}[u(x_{i+1}) - 2u(x_i) + u(x_{i-1})] - \frac{9}{8h}[u'(x_{i+1}) - u'(x_{i-1})] + \frac{1}{8}[u''(x_{i+1}) + u''(x_{i-1})] + \mathcal{O}(h^6), \quad (14)$$

respectively.

Let $v_i \approx v(x_i)$ for an arbitrary function $v(x)$. Dropping the truncated errors in (13) and (14), the sixth-order CCD formulas related to the first and second derivatives are given as follows,

$$\frac{7}{16}(u'_{i+1} + u'_{i-1}) + u'_i - \frac{h}{16}(u''_{i+1} - u''_{i-1}) - \frac{15}{16h}(u_{i+1} - u_{i-1}) = 0 \quad (15)$$

and

$$\frac{9}{8h}(u'_{i+1} - u'_{i-1}) + u''_i - \frac{1}{8}(u''_{i+1} + u''_{i-1}) + \frac{3}{h^2}(u_{i+1} - 2u_i + u_{i-1}) = 0, \quad (16)$$

respectively, where x_i are interior points, $i = 1, 2, \ldots, M-1$.

For periodic boundaries ($u_0 = u_M$, $u'_0 = u'_M$, and $u''_0 = u''_M$), the formulas (15) and (16) hold for $i = 0$. Therefore, the system of (15) and (16) is well-posed and sufficient to deliver the desired results. For nonperiodic boundary problems, in order to keep three-point structure at the two boundaries x_0 and x_M, a pair of fifth-order one-sided CCD schemes are introduced as follows,

$$14u'_0 + 16u'_1 + 2hu''_0 - 4hu''_1 + \frac{1}{h}(31u_0 - 32u_1 + u_2) = 0 \quad (17)$$

and

$$14u'_M + 16u'_{M-1} - 2hu''_M + 4hu''_{M-1} - \frac{1}{h}(31u_M - 32u_{M-1} + u_{M-2}) = 0, \quad (18)$$

respectively; see [1].

On the other hand, the discretized forms of the equation (9) and boundary condition (10) are written as

$$\alpha_i u''_i + \beta_i u'_i + \gamma_i u_i = f_i, \ \ i = 0, 1, \ldots, M, \quad (19)$$

and

$$\zeta_1(0)u_0 + \zeta_2(0)u'_0 = c(0), \ \ \zeta_1(L)u_M + \zeta_2(L)u'_M = c(L). \quad (20)$$

Now we organize formulas (15)–(20) (the CCD method for (9) and (10)) into a triple-tridiagonal system, which is a well-posed system consisting of $3(M+1)$ equations with $3(M+1)$ unknowns (u_i, u'_i, u''_i, for $i = 0, 1, \ldots, M$). Furthermore, since the coefficient matrix of the system possesses a triple-tridiagonal structure, it can be efficiently solved by two steps: triple-forward elimination and triple-backward substitution; see more details in [1].

We remark that though the fifth-order boundary conditions are exploited at boundaries, numerical experiments show that the sixth-order accuracy of the CCD method is guaranteed; see [1, 13].

2.2. Implementation of the CCD-ADI method

To derive our computation scheme, the domain Ω in (1) is divided into a uniform grid with mesh sizes Δx and Δy, and grid numbers M_x and M_y, in x- and y-directions, respectively. We denote $v_{j,k}^n$ as an approximation of $v(x_j, y_k, t_n)$ for an arbitrary function $v(x, y, t)$. In (8), we drop the truncated error term and then have

$$\left(1 - \frac{\Delta t}{2}\mathcal{L}_x\right)\left(1 - \frac{\Delta t}{2}\mathcal{L}_y\right) u_{j,k}^{n+1} = \left(1 + \frac{\Delta t}{2}\mathcal{L}_x\right)\left(1 + \frac{\Delta t}{2}\mathcal{L}_y\right) u_{j,k}^{n} + \Delta t S_{j,k}^{n+1/2}, \tag{21}$$

where $j = 0, 1, \ldots, M_x$, and $k = 0, 1, \ldots, M_y$.

By introducing an intermediate variable u^* and applying the D'Yakonov ADI-like scheme [10], (21) can be written as

$$\left(1 - \frac{\Delta t}{2}\mathcal{L}_x\right) u_{j,k}^{*} = \left(1 + \frac{\Delta t}{2}\mathcal{L}_x\right)\left(1 + \frac{\Delta t}{2}\mathcal{L}_y\right) u_{j,k}^{n} + \Delta t S_{j,k}^{n+1/2}, \tag{22}$$

$$\left(1 - \frac{\Delta t}{2}\mathcal{L}_y\right) u_{j,k}^{n+1} = u_{j,k}^{*}. \tag{23}$$

Here both of (22) and (23) are one dimensional problems which can be solved by the CCD method. More precisely, combined with the sixth-order CCD formulas (15) and (16), along with the boundary CCD formulas (17) and (18), replacing h by Δx and Δy respectively, equations (22) and (23) are solved with the accuracy of $\mathcal{O}(\Delta x^6 + \Delta y^6 + \Delta t^2)$.

Nevertheless, it is nontrivial to compute the right-hand side of (22) as all first and second derivatives of $u_{j,k}^n$ with $j,\ k = 0, 1, \ldots, M_x\,(M_y)$ are required. Therefore, in the implementation of the CCD-ADI method, we need to compute those derivatives with higher order accuracy beforehand. In the following, we introduce how to calculate the first and second derivatives for a given function by the CCD method.

For the periodic boundary case, the linear system of (15) and (16) is sufficient to calculate all u_i' and u_i'', provided that u_i, $i = 0, \ldots, M$, are given. For the nonperiodic boundary case, however, there are only $2(M-1)$ equations in (15) and (16). Besides the boundary CCD formulas (17) and (18), we also need two additional boundary CCD formulas (see [1]),

$$u_0' + 2u_1' - hu_1'' = -\frac{1}{2h}(7u_0 - 8u_1 + u_2) \tag{24}$$

and

$$u_M' + 2u_{M-1}' + hu_{M-1}'' = \frac{1}{2h}(7u_M - 8u_{M-1} + u_{M-2}), \tag{25}$$

to compute all $2(M+1)$ unknowns u_i' and u_i''.

The following algorithm gives a general procedure in the implementation of the CCD-ADI method (22) and (23) for the 2D unsteady convection-diffusion equation (1).

Algorithm 1: Implementation of the CCD-ADI method

1. Do $j = 0, 1, \ldots, M_x$
   Compute $(u_y^0)_{j,k}$ and $(u_{yy}^0)_{j,k}$ by (15)–(18) and (24)–(25) for $k = 0, 1, \ldots, M_y$
2. Do $n = 0, 1, \ldots, N-1$
   (a) Compute the right-hand side of (22) for all mesh points
      i. $g_{j,k}^n := u_{j,k}^n + \Delta t[b(u_{yy})_{j,k}^n - q(u_y)_{j,k}^n]/2$
      ii. Calculate $(g_x)_{j,k}^n$ and $(g_{xx})_{j,k}^n$ by (15)–(18) and (24)–(25)
      iii. $f_{j,k}^n := g_{j,k}^n + \Delta t[a(g_{xx})_{j,k}^n - p(g_x)_{j,k}^n]/2 + \Delta t S_{j,k}^{n+1/2}$
   (b) Compute the boundary conditions $u_{j,k}^*$ in (22) for $j = 0,\ M_x$ and $k = 0, 1, \ldots, M_y$
      i. Calculate $(u_y)_{j,k}^{n+1}$ and $(u_{yy})_{j,k}^{n+1}$ by (15)–(18) and (24)–(25)
      ii. $u_{j,k}^* := u_{j,k}^{n+1} - \Delta t[b(u_{yy})_{j,k}^{n+1} - q(u_y)_{j,k}^{n+1}]/2$
   (c) Solve (22), or $[1 - (\Delta t/2)\mathcal{L}_x]\, u_{j,k}^* = f_{j,k}^n$, with the CCD scheme (15)–(20)
   (d) Solve (23), or $[1 - (\Delta t/2)\mathcal{L}_y]\, u_{j,k}^{n+1} = u_{j,k}^*$, with the CCD scheme (15)–(20)

We note that the central finite difference scheme is employed in (5) for the temporal discretization. Hence the truncation error term in (5) has the asymptotic expansion as follows,

$$\frac{u^{n+1} - u^n}{\Delta t} - \frac{1}{2}\left(\mathcal{L}_x + \mathcal{L}_y\right)\left(u^{n+1} + u^n\right) - S^{n+1/2} = C_1 \Delta t^2 + C_2 \Delta t^4 + C_3 \Delta t^6 + \cdots,$$

where C_1, C_2 and C_3 are independent of Δt. Therefore, in practice, as in [8], the famous Richardson extrapolation scheme can be implemented in the proposed method to improve the temporal accuracy at the final time step up to fourth order; see [2, 8] for its formula and details.

3. Stability Analysis

Now we study the stability of the ADI-CCD method by von Neumann linear stability analysis. Assume that u is periodic in both x- and y-direction and $S \equiv 0$. At grid node (j,k), let

$$u_{j,k}^n = \xi^n e^{\mathbf{i}(w_x j + w_y k)},\ (u_x)_{j,k}^n = \eta_x^n e^{\mathbf{i}(w_x j + w_y k)},$$

$$(u_{xx})_{j,k}^n = \mu_x^n e^{\mathbf{i}(w_x j + w_y k)},\ (u_y)_{j,k}^n = \eta_y^n e^{\mathbf{i}(w_x j + w_y k)},\ (u_{yy})_{j,k}^n = \mu_y^n e^{\mathbf{i}(w_x j + w_y k)},$$

where $\mathbf{i} = \sqrt{-1}$, ξ^n, η_x^n, μ_x^n, η_y^n, μ_y^n are amplitudes at time level n, and w_x and w_y are phase angles in x- and y- directions, respectively.

Lemma 1. *According to* (15) *and* (16)*, we have*

$$\begin{cases} \eta_x^n = \dfrac{\xi^n B_x}{\Delta x A_x}\mathbf{i}, \\ \mu_x^n = \dfrac{\xi^n C_x}{\Delta x^2 A_x}, \end{cases} \quad \begin{cases} \eta_y^n = \dfrac{\xi^n B_y}{\Delta y A_y}\mathbf{i}, \\ \mu_y^n = \dfrac{\xi^n C_y}{\Delta y^2 A_y}, \end{cases} \tag{26}$$

where $A_{x(y)} = 20\cos w_{x(y)} + 2\cos^2 w_{x(y)} + 23,\ B_{x(y)} = 9\sin w_{x(y)}(\cos w_{x(y)} + 4),$ *and* $C_{x(y)} = 3(8\cos w_{x(y)} + 11\cos^2 w_{x(y)} - 19).$

Proof:

We only prove the first formula in (26). The proof for the second formula is analogously obtained.

For all j, k, substituting $u_{j,k}^n$, $(u_x)_{j,k}^n$ and $(u_{xx})_{j,k}^n$ into (15) and (16), we have

$$\begin{cases} \frac{7}{16}\eta_x^n e^{\mathbf{i}(w_x j + w_y k)}(e^{\mathbf{i}w_x} + e^{-\mathbf{i}w_x}) + \eta_x^n e^{\mathbf{i}(w_x j + w_y k)} - \frac{\Delta x}{16}\mu_x^n e^{\mathbf{i}(w_x j + w_y k)}(e^{\mathbf{i}w_x} - e^{-\mathbf{i}w_x}) \\ = \frac{15}{16\Delta x}\xi^n e^{\mathbf{i}(w_x j + w_y k)}(e^{\mathbf{i}w_x} - e^{-\mathbf{i}w_x}), \\ \frac{9}{8\Delta x}\eta_x^n e^{\mathbf{i}(w_x j + w_y k)}(e^{\mathbf{i}w_x} - e^{-\mathbf{i}w_x}) - \frac{1}{8}\mu_x^n e^{\mathbf{i}(w_x j + w_y k)}(e^{\mathbf{i}w_x} + e^{-\mathbf{i}w_x}) + \mu_x^n e^{\mathbf{i}(w_x j + w_y k)} \\ = \frac{3}{\Delta x^2}\xi^n e^{\mathbf{i}(w_x j + w_y k)}(e^{\mathbf{i}w_x} - 2 + e^{-\mathbf{i}w_x}). \end{cases}$$

By Euler's formula, we have $e^{\mathbf{i}w_x} + e^{-\mathbf{i}w_x} = 2\cos w_x$ and $e^{\mathbf{i}w_x} - e^{-\mathbf{i}w_x} = 2\mathbf{i}\sin w_x$. After rearranging terms, we obtain

$$\begin{cases} (1 + \frac{7}{8}\cos w_x)\eta_x^n - \mathbf{i}\frac{\Delta x}{8}\sin w_x \mu_x^n = \mathbf{i}\frac{15}{8\Delta x}\xi^n \sin w_x, \\ \mathbf{i}\frac{9}{4\Delta x}\sin w_x \eta_x^n + (1 - \frac{1}{4}\cos w_x)\mu_x^n = \frac{6}{\Delta x^2}\xi^n(\cos w_x - 1). \end{cases}$$

Solving above linear system, we have

$$\begin{cases} \eta_x^n = \frac{9\xi^n \sin w_x(\cos w_x + 4)}{\Delta x(20\cos w_x + 2\cos^2 w_x + 23)}\mathbf{i} = \frac{\xi^n B_x}{\Delta x A_x}\mathbf{i}, \\ \mu_x^n = \frac{3\xi^n(8\cos w_x + 11\cos^2 w_x - 19)}{\Delta x^2(20\cos w_x + 2\cos^2 w_x + 23)} = \frac{\xi^n C_x}{\Delta x^2 A_x}. \end{cases}$$

□

Based on Lemma 1, the unconditional stability of the CCD-ADI method is led in the following theorem.

Theorem 1. *The amplification factor* ξ *of the CCD-ADI method satisfies* $|\xi| \le 1$.

Proof: Substituting expressions of $(u_x)^n_{j,k}$, $(u_{xx})^n_{j,k}$, $(u_y)^n_{j,k}$, $(u_{yy})^n_{j,k}$ and $(u)^n_{j,k}$ into (21), by (26) in Lemma 1, we have

$$\begin{aligned}\xi &= \frac{u^{n+1}_{j,k}}{u^n_{j,k}} \\ &= \left[\frac{1+\frac{\Delta t}{2}\left(\frac{aC_x}{A_x\Delta x^2}-\frac{pB_x}{A_x\Delta x}\mathbf{i}\right)}{1-\frac{\Delta t}{2}\left(\frac{aC_x}{A_x\Delta x^2}-\frac{pB_x}{A_x\Delta x}\mathbf{i}\right)}\right]\left[\frac{1+\frac{\Delta t}{2}\left(\frac{bC_y}{A_y\Delta y^2}-\frac{qB_y}{A_y\Delta y}\mathbf{i}\right)}{1-\frac{\Delta t}{2}\left(\frac{bC_y}{A_y\Delta y^2}-\frac{qB_y}{A_y\Delta y}\mathbf{i}\right)}\right] \\ &\equiv g_x(w_x)g_y(w_y).\end{aligned}$$

Since

$$g_x(w_x) = \frac{1+\frac{\Delta t}{2}\left(\frac{aC_x}{A_x\Delta x^2}-\frac{pB_x}{A_x\Delta x}\mathbf{i}\right)}{1-\frac{\Delta t}{2}\left(\frac{aC_x}{A_x\Delta x^2}-\frac{pB_x}{A_x\Delta x}\mathbf{i}\right)} = \frac{\left(1+\frac{aC_x\Delta t}{2A_x\Delta x^2}\right)-\frac{pB_x\Delta t}{2A_x\Delta x}\mathbf{i}}{\left(1-\frac{aC_x\Delta t}{2A_x\Delta x^2}\right)+\frac{pB_x\Delta t}{2A_x\Delta x}\mathbf{i}},$$

where the imaginary parts of the numerator and denominator are the same, we only consider their real parts.

Note from (26) that $A_x > 0$, $A_y > 0$ and $C_x \leq 0$, $C_y \leq 0$, hence

$$1+\frac{aC_x\Delta t}{2A_x\Delta x^2} \leq 1-\frac{aC_x\Delta t}{2A_x\Delta x^2} \quad \text{and} \quad 1+\frac{bC_y\Delta t}{2A_y\Delta y^2} \leq 1-\frac{bC_y\Delta t}{2A_y\Delta y^2}$$

which imply $|g_x(w_x)| \leq 1$ and $|g_y(w_y)| \leq 1$. Thus $|\xi| = |g_x(w_x)g_y(w_y)| \leq 1$. □

From Theorem 1, we conclude that the CCD-ADI method is unconditionally stable.

4. Numerical experiments

In this section, we test three problems and present the numerical results by the proposed CCD-ADI method. For comparisons of high order accuracy, we also show the numerical results by the HOC-ADI method [5] and the RHOC-ADI method [14]. All experiments are performed under Matlab 7.10 on a Dell Vostro 260s computer with 3.1GHz Intel Core i5-2400 CPU and 4GB RAM.

Example 1.

Consider a pure diffusion ($p = q = 0$) equation in the unit square domain $[0, 1] \times [0, 1]$ with diffusion coefficients $a = b = 1$, and the analytic solution is given by

$$u(x, y, t) = e^{-2\pi^2 t}\sin(\pi x)\sin(\pi y).$$

The initial condition (2), the Dirichlet boundary condition (3), and the source term are directly taken from this solution. This test problem was in [5, 14].

The numerical results obtained for *Example 1* with the CCD-ADI scheme, the RHOC-ADI scheme, and the HOC-ADI scheme under a uniform grid ($\Delta x = \Delta y = h$) with different mesh sizes and their accuracies compared under the relative L^2-norm error of the numerical solution with respect to the analytic solution are presented in Table 1. We choose the time increment $\Delta t = 1/1024$ and the final time $T = 1$ for the verification of spatial accuracy. Meanwhile, the Richardson extrapolation method is exploited to increase the temporal accuracy to fourth order at the final time step. The use of "Rate" (Rate = $\ln(err1/err2)$) indicates the convergence rate of each computation scheme, where $err1$ and $err2$ are relative L^2-norm errors with the mesh sizes h and $h/2$, respectively. Let "CPU" be the total CPU time in seconds for solving the discretized system of (1). We note that the present CCD-ADI scheme produces much more accurate results in comparison with the RHOC-ADI scheme and the HOC-ADI scheme.

Table 1: L^2-norm errors and convergence rate in space with $T = 1$ and $\Delta t = 1/1024$.

M	CCD-ADI			HOC-ADI			RHOC-ADI		
	Error	Rate	CPU	Error	Rate	CPU	Error	Rate	CPU
4	8.820×10^{-3}	—	8.004	3.255×10^{-2}	—	1.571	3.255×10^{-2}	—	1.642
8	6.787×10^{-5}	7.022	24.56	1.969×10^{-3}	4.046	6.722	1.969×10^{-3}	4.046	7.046
16	3.899×10^{-7}	7.444	85.04	1.225×10^{-4}	4.007	28.57	1.225×10^{-4}	4.007	29.86
32	1.554×10^{-9}	7.970	320.7	7.661×10^{-6}	3.999	118.5	7.661×10^{-6}	3.999	124.3

Example 2.

Consider (1) in $[0, 2] \times [0, 2]$ with an analytic solution

$$u(x, y, t) = \frac{1}{4t + 1} \exp\left(-\frac{(x - pt - 0.5)^2}{a(4t + 1)} - \frac{(y - qt - 0.5)^2}{b(4t + 1)}\right),$$

which was shown in [5, 9, 14]. As in *example 1*, the initial condition, the Dirichlet boundary condition, and the source term are directly taken from the analytic solution.

Example 2 is solved under a uniform grid ($\Delta x = \Delta y = h = 0.02$) to show how the cell Reynolds number affects the numerical solutions of (1) by different schemes, where cell Reynolds number $Pe_x = p\Delta x/a$ is defined for the x-direction and $Pe_y = q\Delta y/b$ is defined for the y-direction respectively; see [14]. Since $a = b$ and $p = q$, the cell Reynolds number can be simply defined as $Pe = ph/a$.

Figure 1 shows L^2-norm errors of the discretized solutions when $Pe = 2$ with respect to the exact solution at each time step. The present CCD-ADI scheme obviously produces a significantly smaller error than other schemes.

Figure 2 and Figure 3 contain contour plots of the analytic and computed pulses in the sub-region $1.2 \leq x, y \leq 1.8$ for each test. In the case of $Pe = 2$, accuracies of three schemes show little difference. Numerical solutions obtained from the present CCD-ADI, the RHOC-ADI, and the HOC-ADI schemes are compared with the exact solution at the final time step ($t = 1$) in Figure 2. Solutions obtained from these three schemes (Figure 1(a), (b) and (c) correspond to the present CCD-ADI, HOC-ADI, and RHOC-ADI schemes, respectively) capture the moving pulse very well, yielding pulses centered at (1.5, 1.5) and almost visually indistinguishable from the exact solution (Figure 2(d)).

In the high cell Reynolds number case ($Pe = 2000$), Figure 3 shows contour plots of the numerical and exact solutions at $t = 0.001$. The present CCD-ADI and RHOC-ADI schemes produce the approximations in good agreement with the exact solution in terms of amplitude and phase (see Figure 3(a) and (c)), while considerable difference between the HOC-ADI solution and the exact solution is clearly exhibited in Figure 3(b). As mentioned in [16], the enhanced numerical dissipation makes the HOC-ADI scheme unattractive for direct numerical simulations or large eddy simulations of turbulent flows.

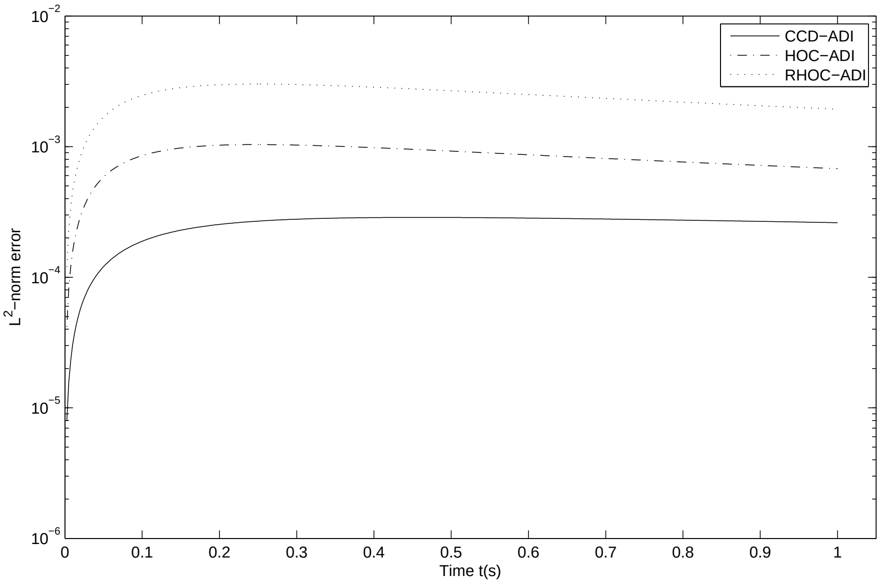

Figure 1: Comparison of the L^2-norm errors produced by three schemes at each time step.

Example 3.

In order to show the advantages of the proposed CCD-ADI method further, we constructed a new test problem, whose analytic solution is

$$u(x, y, t) = e^{-(a^3+b^3)t} \sin(ax + by).$$

Consider (1) in the square domain $[0, 2] \times [0, 2]$ with nonzero convection velocities. The Dirichlet boundary condition and initial condition are taken from the analytic solution, and the source term is

$$S(x, y, t) = (ap + bq)e^{-(a^3+b^3)t} \cos(ax + by).$$

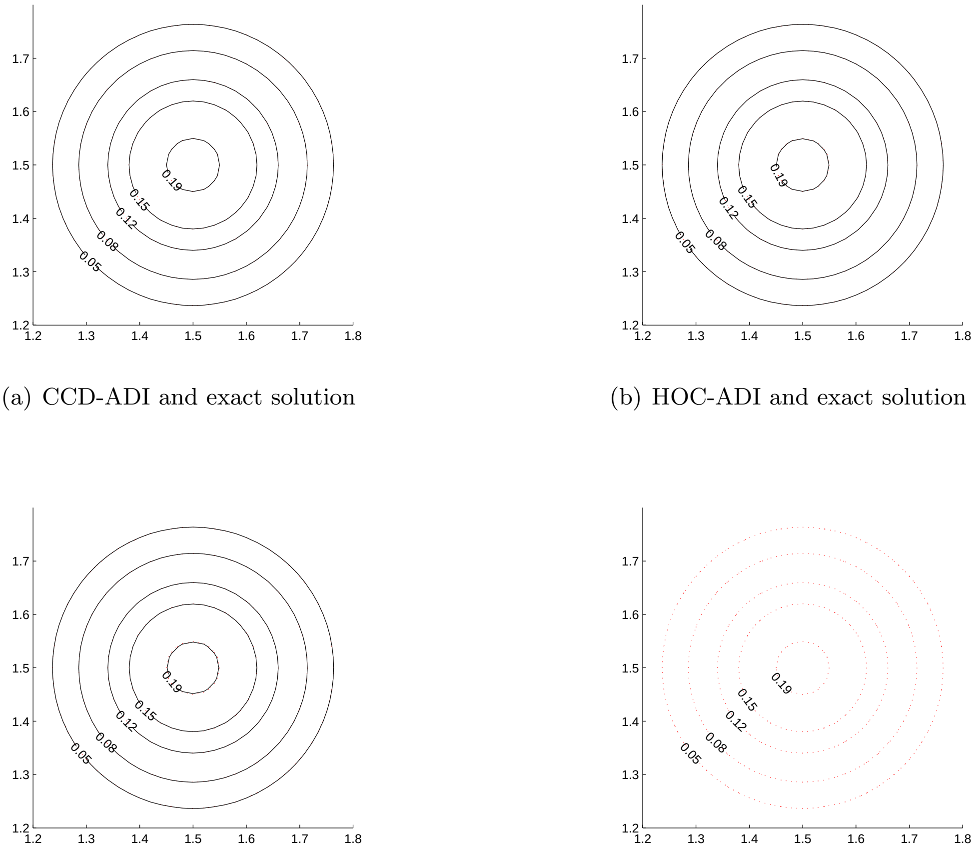

(a) CCD-ADI and exact solution

(b) HOC-ADI and exact solution

(c) RHOC-ADI and exact solution

(d) exact solution

Figure 2: Contour plots of the pulse in the sub-region $1.2 \leq x, y \leq 1.8$ at $t = 1$: (a) exact and the present ADI, (b) exact and the HOC-ADI, (c) exact and the RHOC-ADI, (d) exact [$Pe = 2$, $\Delta t = 2.5 \times 10^{-3}$]. Dotted contour lines in (a)-(d) correspond to exact solution.

The numerical results obtained for *Example 3* with the present CCD-ADI scheme, the RHOC-ADI scheme, and the HOC-ADI scheme, under a uniform grid ($\Delta x = \Delta y$) with different time increments, are presented in Table 2. The Richardson extrapolation method is employed to increase the temporal accuracy to fourth order at the final time step. To study the superiority of the present CCD-ADI scheme more clearly in the case of high cell Reynolds number, we set diffusion coefficients $a = b = 1$ and let convection coefficients become gradually dominant; i.e., $p = q = 64$, 640, 6400, and 64000.

In Table 2, $\Delta x = \Delta y = 1/64$ and the final time $T = 1$ are chosen for the verifications of fourth-order accuracy in time. The convergence rates are estimated using $\ln(err1/err2)$, where $err1$ and $err2$ denote the L^2-norm errors with time step sizes $2\Delta t$ and Δt, respectively. From Table 2, a remarkable characteristic of the CCD-ADI scheme is that, as the convection

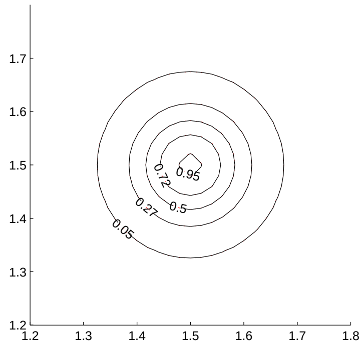

(a) CCD-ADI and exact solution

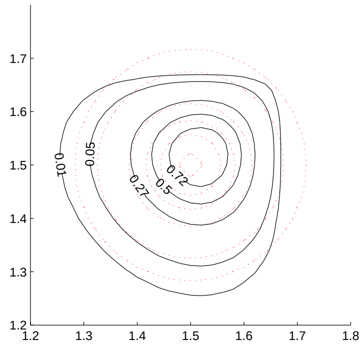

(b) HOC-ADI and exact solution

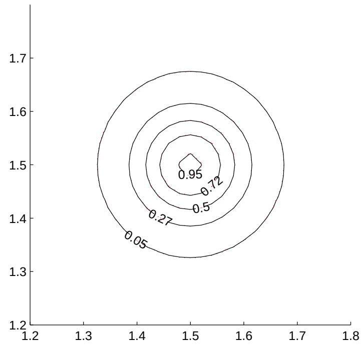

(c) RHOC-ADI and exact solution

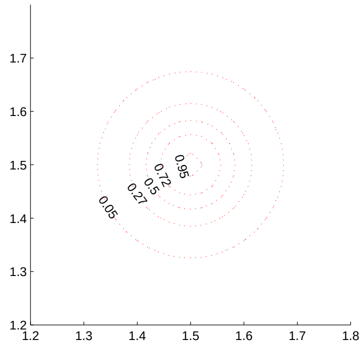

(d) exact solution

Figure 3: Contour plots of the pulse in the sub-region $1.2 \le x, y \le 1.8$ at $t = 0.001$: (a) exact and the present ADI, (b) exact and the HOC-ADI, (c) exact and the RHOC-ADI, (d) exact [$Pe = 2000$, $\Delta t = 2.5 \times 10^{-6}$]. Dotted contour lines in (a)-(d) correspond to exact solution.

coefficients are generally increased, the magnitudes of the L^2-norm errors remain almost unchanged, while the magnitudes of the L^2-norm errors of the HOC-ADI scheme and the RHOC-ADI scheme are significantly affected. In particular, from the last two sets of results ($p = q = 6400$ and $p = q = 64000$) in Table 2, the HOC-ADI and RHOC-ADI schemes become very unreliable.

5. Concluding remarks

In this paper, we developed a CCD-ADI method for solving 2D unsteady convection-diffusion problems. The proposed method is sixth order accurate in space and second order accurate in time. The unconditional stability of the CCD-ADI method is verified by discrete Fourier analysis. Numerical experiments have been carried out for solving the 2D unsteady

Table 2: L^2-norm errors and temporal convergence rates with $T = 1$, $\Delta x = \Delta y = 1/64$ and different convection velocities.

$p = q$	$\triangle t$	CCD-ADI		HOC-ADI		RHOC-ADI	
		Error	Rate	Error	Rate	Error	Rate
64	T/16	2.8827×10^{-6}	—	3.5519×10^{-2}	—	3.5519×10^{-2}	—
	T/32	1.8904×10^{-7}	3.9307	2.3016×10^{-3}	3.9478	2.3019×10^{-3}	3.9477
	T/64	9.5528×10^{-9}	4.3066	1.2412×10^{-4}	4.2129	1.2407×10^{-4}	4.2136
	T/128	5.6711×10^{-10}	4.0742	7.4570×10^{-6}	4.0570	7.3961×10^{-6}	4.0682
640	T/16	3.2712×10^{-6}	—	9.6356×10^{-1}	—	9.6390×10^{-1}	—
	T/32	3.0858×10^{-7}	3.4061	2.9010×10^{-1}	1.7318	3.7066×10^{-1}	1.6991
	T/64	1.4031×10^{-8}	4.4590	1.5592×10^{-2}	4.2177	1.8529×10^{-2}	4.0020
	T/128	7.2330×10^{-10}	4.2778	8.6397×10^{-4}	4.1737	9.1505×10^{-4}	4.3398
6400	T/16	1.8620×10^{-7}	—	6.0198×10^{0}	—	2.2879×10^{1}	—
	T/32	9.6998×10^{-8}	0.9409	3.4644×10^{0}	0.7971	3.4568×10^{0}	2.7265
	T/64	1.3590×10^{-8}	2.8354	4.0331×10^{-1}	3.1026	1.1897×10^{0}	1.4163
	T/128	9.2893×10^{-10}	3.8709	1.1147×10^{-1}	1.8552	8.3908×10^{-2}	3.9481
64000	T/16	8.3888×10^{-8}	—	2.6460×10^{-1}	—	1.6708×10^{3}	—
	T/32	4.7360×10^{-8}	0.8248	2.6599×10^{-1}	-0.0076	2.4712×10^{2}	2.7572
	T/64	8.1722×10^{-9}	2.5349	2.7086×10^{-1}	-0.0262	8.1580×10^{1}	1.5989
	T/128	5.1498×10^{-10}	3.9881	2.7735×10^{-1}	-0.0342	5.7014×10^{0}	3.9853

convection-diffusion equations. They show that the proposed CCD-ADI method can achieve higher order accuracy and also keep the lower CPU cost. In addition, for extremely convection dominated problems, the proposed method still preserve the higher order accuracy, which is much superior to other HOC-ADI schemes. Furthermore, the CCD-ADI method is easily extendible to multi-dimensional problems and also can be implemented for problems with variable coefficients if we leave out the stability analysis. In our future works, we will exploit this strategy of combining CCD method and ADI technique for solving nonlinear unsteady problems.

Acknowledgements

The authors would like to thank Guang-hua Gao for her helpful discussions. We are also grateful to the anonymous referees for their useful comments and suggestions.

References

[1] P. Chu, C. Fan, *A three-point combined compact difference scheme*, Journal of Computational Physics, 140 (1998), pp. 370–399.

[2] M. Garbey, W. Shyy, *A least square extrapolation method for improving solution accuracy of PDE computations*, Journal of Computational Physics, 186 (2003), pp. 1–23.

[3] R. Hirsh, *Higher order accurate difference solutions of fluid mechanics problems by a compact differencing technique*, Journal of Computational Physics, 19 (1975), pp. 90–109.

[4] S. Karaa, *An accurate LOD scheme for two-dimensional parabolic problems*, Applied Mathematics and Computation, 170 (2005), pp. 886–894.

[5] S. Karaa, J. Zhang, *High order ADI method for solving unsteady convection-diffusion problems*, Journal of Computational Physics, 198 (2004), pp. 1–9.

[6] J. C. Kalita, D. C. Dalal, A. K. Dass, *A class of higher order compact schemes for the unsteady two-dimensional convection-diffusion equation with variable convection coefficients*, Int. J. Numer. Methods Fluids, 38 (2002), pp. 1111–1131.

[7] J. Li, Y. Chen, G. Liu, *High-order compact ADI methods for parabolic equations*, Computers and Mathematics with Applications, 52 (2006), pp. 1343–1356.

[8] H. Liao, Z. Sun, *Maximum norm error bounds for ADI and compact ADI methods for solving parabolic equations*, Numerical Methods for Partial Differential Equations, 26 (2010), pp. 37–60.

[9] B. Noye, H. Tan, *Finite difference methods for solving the two dimensional advection-diffusion equation*, International Journal for Numerical Methods in Fluids, 9 (1989), pp. 75–89.

[10] D. Peaceman, H. Rachford, *The numerical solution of parabolic and elliptic differential equations*, Journal of the Society for Industrial and Applied Mathematics, 3 (1955), pp. 28–41.

[11] P. J. Roach, *Computational Fluid Dynamics*, Hermosa, Albuquerque, NM, 1976.

[12] W. Spotz, *High-Order Compact Finite Difference Schemes for Computational Mechanics*, PhD Thesis, University of Texas at Austin,1995.

[13] H. Sun, J. Zhang, *A high-order finite difference discretization strategy based on extrapolation for convection diffusion equations*, Numerical Methods for Partial Differential Equations, 20 (2004), pp. 18–32.

[14] Z. Tian, *A rational high-order compact ADI method for unsteady convection-diffusion equations*, Computer Physics Communications, 182 (2011), pp. 649–662.

[15] Z. Tian, Y. Ge, *A fourth-order compact ADI method for solving two-dimensional unsteady convection-diffusion problems*, J. Comput. Appl. Math., 198 (2007), pp. 268–286.

[16] D. You, *A high-order Padé ADI method for unsteady convection-diffusion equations*, Journal of Computational Physics, 214 (2006), pp. 1–11.

[17] J. Zhang, *An explicit fourth-order compact finite difference scheme for three dimensional convection-diffusion equation*, Commun. Numer. Methods Engrg., 14 (1998), pp. 209–218.